Article

J. Biol. Regul. Homeost. Agents. 2024; 38(7): 5473–5487
https://doi.org/10.23812/j.biol.regul.homeost.agents.20243807.439

Synthesis and Characterization of Mesoporous SBA-15 as Carriers to Improve the Rutin Dissolution Rate

Sheeba Francis Roselet[1,*], Sultan Alshehri[2], Kuntal Das[3], Shanmugam Vippamakula[4], Amro Mohammed Sawadi Khormi[5], Mutlaq Eidhah M. Almalki[6], Fuzail Ahmad[7], Syed Imam Rabbani[8], Syed Mohammed Basheeruddin Asdaq[9,*]

[1]Department of Pharmaceutics, Mallige College of Pharmacy, 560090 Bangalore, Karnataka, India
[2]Department of Pharmaceutics, College of Pharmacy, King Saud University, 11451 Riyadh, Saudi Arabia
[3]Department of Pharmacognosy and Phytochemistry, Mallige College of Pharmacy, 560090 Bangalore, Karnataka, India
[4]Department of Pharmaceutics, MB School of Pharmaceutical Sciences, Mohan Babu University, 517102 A. Rangampet, Tirupati, India
[5]Department of Pharmacy, King Saud University Medical City, 12371 Riyadh, Saudi Arabia
[6]Department of Pharmaceutical Sciences, King Saud University, 11451 Riyadh, Saudi Arabia
[7]Department of Respiratory Therapy, College of Applied Sciences, AlMareefa University, 12371 Riyadh, Saudi Arabia
[8]Department of Pharmacology and Toxicology, College of Pharmacy, Qassim University, 51452 Buraydah, Saudi Arabia
[9]Department of Pharmacy Practice, College of Pharmacy, AlMaarefa University, 13713 Riyadh, Saudi Arabia
*Correspondence: sheebagiles@gmail.com (Sheeba Francis Roselet); sasdag@um.edu.sa; sasdaq@gmail.com (Syed Mohammed Basheeruddin Asdaq)
Submitted: 20 February 2024 Revised: 5 April 2024 Accepted: 9 April 2024 Published: 1 July 2024

Background: Due to its low water solubility, Rutin, a crystalline medication used to treat a variety of conditions, has a limited rate of dissolution when given in gastrointestinal fluids. The present study planned to formulate and characterize Rutin using mesoporous silica material (SBA-15) as well as to determine the *in-vitro* dissolution properties.

Methods: Rutin was formulated using mesoporous silica material such as SBA-15. Particle size distribution analysis, fourier transform-infrared (FT-IR) spectroscopy, scanning electron microscopy, and X-ray diffraction were used to characterize the compound in the complex. Rutin's solubility and *in-vitro* release characteristics were assessed. Furthermore, the dissolution data (DD) Solver Excel add-in software was used to evaluate several mathematical models to interpret the Rutin dissolution kinetics from the mesoporous materials.

Results: Differential scanning calorimetry was used to confirm Rutin's amorphous state, which resulted in a significantly higher rate of dissolution than pure crystalline Rutin. The release of the drug from the Rutin/SBA-15 complex was well-simulated by the Weibull model. Notably, the SBA-15 carrier-mediated complex of Rutin exhibited the highest drug loading and dissolution rate, showing promising potential for enhancing Rutin bioavailability.

Conclusion: The findings suggested that Rutin/SBA-15 could be easily incorporated into conventional oral pharmaceutical dosage forms such as capsules and therefore can be utilized for treating ailments such as allergies, inflammation, tumors, infections, protozoal diseases, and spasms. To assess the Rutin/SBA-15 complex's *in-vivo* pharmacokinetic performance and appropriateness for a range of pharmacological actions, more investigation is required.

Keywords: drug screening; formulation; Rutin; mesoporous SBA-15; characterization; dissolution properties

Introduction

Rutin is reported to exhibit some important pharmacological properties such as antibacterial, antiprotozoal, anticancer, anti-inflammatory, antiallergic, antiviral, cytoprotective, vasoactive, hypolipidemic, antiplatelet, antispasmodic and antihypertensive [1]. In the food sector, Rutin is frequently utilized as a stabilizer, colorant, antioxidant, and preservative. It is naturally derived from many sources in plants. Additionally, several herbal medicines and multivitamin supplements contain Rutin as a necessary ingredient [1–3]. Still, in many cases, substantial doses of Rutin and prolonged administration times are required to provide the best possible therapeutic outcome. The medication's low water solubility (around 0.125 g/L), which results in sluggish rates of dissolution in the gastrointestinal fluids, is the primary source of this issue [4,5]. Besides, the pace at which the drug is absorbed is reported to be hampered by low plasma drug levels [5].

Therefore, one of the biggest obstacles to developing a more effective therapy with Rutin for various pharmacological effects is to increase its water solubility and dissolution rate.

To enhance Rutin's solubility and rate of dissolution, various technologies were employed, including such as solid dispersions [6], complexation with beta-

Journal of
BIOLOGICAL REGULATORS
and Homeostatic Agents

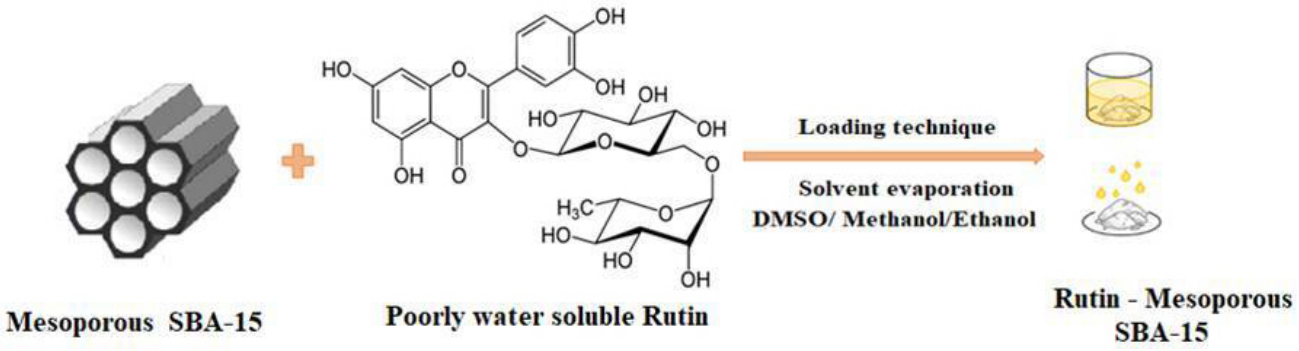

Fig. 1. Schematic illustration of Rutin loaded into mesoporous SBA-15. DMSO, dimethyl sulfoxide.

cyclodextrins [7–9], nanostructured liquisolid [10], formulation of Rutin-frankincense tablets [11], trihydrate emulgels [12], lipophilic prodrug of Rutin [13] as well as nanoparticles form of Rutin [14,15]. These methods often include multiple production processes, various ingredients, and the use of organic solvents. However, structured mesoporous silica particles offer a potential substitute due to their advantageous qualities that enhance drug dispersion as well as their biocompatibility and lack of toxicity [12,14].

In the above-mentioned techniques, the particles' wide surface area, sizable pore volume, and well-organized pore structure all help to increase the rate of drug dissolution and solubility [10]. But ordered mesoporous silica materials are said to have better methods than polymers, which are commonly used to promote solubility, in terms of heat, pH, and storage stability [16]. Furthermore, when compared to the crystalline state, the amorphous state of drug molecules found in mesoporous is well stabilized and the presence of porous structure in these materials is known to increase the drug's solubility along with better rate of dissolution [16,17].

Because of its dual-porosity structure, which comprises linked mesopores and micropores that are said to give hydrothermal and thermal stability, SBA-15 stands out from other ordered mesoporous silica particles [16]. As per earlier research, SBA-15 has been extensively examined for its potential as a delivery system for low water-soluble drugs such as ibuprofen, fenofibrate, glibenclamide, ezetimibe, indomethacin, itraconazole, telmisartan, and griseofulvin [18]. Furthermore, research conducted on *in-vivo* experimental models has shown that SBA-15 is an efficient carrier of those medications that are poorly soluble in water, such as carbamazepine, fenofibrate, and ketoprofen [19]. These medications can be added to mesoporous silica solids to efficiently lower the particle size and increase the rate of dissolution [18,19]. Considering these data, our study has a novel approach to loading the Rutin into mesoporous silica materials (SBA-15) and evaluating the dissolution rate as well as solubility characteristics of the Rutin/SBA-15 complex using various experimental models.

Materials and Methods

Drugs and Chemicals

Tetraethyl orthosilicate (TEOS, Batch number 0141), Pluronic P123 (Lot # 1587), and Rutin (Sample ID number 1126585) were obtained from Yarrow Chem, Mumbai, India. The solvents methanol (B.N.114), acetic acid (B.N: 699987), hydrochloric acid (Lot # 4857), dimethyl sulfoxide (DMSO, Sample # 593874), and carbon tetra chloride (Batch # 98324) were purchased from Indian Fine Chemicals, Bangalore, India. All reagents were of analytical grade and were employed as received from the supplier.

Synthesis of SBA-15 Ordered Mesoporous Silica Carriers

The synthesis of the SBA-15 silica material was realized according to the protocol proposed by Zhao *et al*. [20] and modified by Belmoujahid *et al*. [21]. SBA-15 was synthesized utilizing Tetraethyl orthosilicate (TEOS) as a silicon source and Pluronic123 as a template. In brief, a defined amount of P123 (8.0 g) was added into 365 mL of 2 M HCl solution (Batch number: 1228, HiMedia Laboratories, Mumbai, India) at 40 °C in a round bottom flask with constant stirring until a clear light blue solution was formed. Then, 17.53 g of TEOS was added dropwise, followed by stirring for 24 h at 40 °C. A white solid was obtained after aging. The obtained solid was filtered and washed thoroughly with distilled water; air dried first at room temperature overnight and after that, the sample was dried in an oven at 80 °C for 5–6 h. Finally, the sample was calcined at 550 °C for 4–6 h for removal of template.

Drug Loading to Mesoporous SBA-15

The solvent evaporation method was used to load Rutin onto SBA-15 as represented in Fig. 1. In this method, the mesoporous SBA-15 was dispersed in a Rutin-containing volatile organic solution such as ethanol (Batch # 1012, SD Fine Chemicals, Mumbai, India), methanol (Batch # 0495, SD Fine Chemicals, Mumbai, India), or DMSO (Batch # 6523, SD Fine Chemicals, Mumbai, India). Then this solution was dried by fast solvent evapo-

Table 1. Solvents used for Rutin loading to mesoporous SBA-15.

Formulation code	Rutin (mg)	Mesoporous SBA-15 (mg)	Drug loading solvent (50 mL)
FD1	100	100	DMSO
FD2	100	150	DMSO
FD3	100	200	DMSO
FE1	100	100	Ethanol
FE2	100	150	Ethanol
FE3	100	200	Ethanol
FM1	100	100	Methanol
FM2	100	150	Methanol
FM3	100	200	Methanol

DMSO, dimethyl sulfoxide; FD, formulation with DMSO solvent; FE, formulation with ethanol; FM, formulation with methanol.

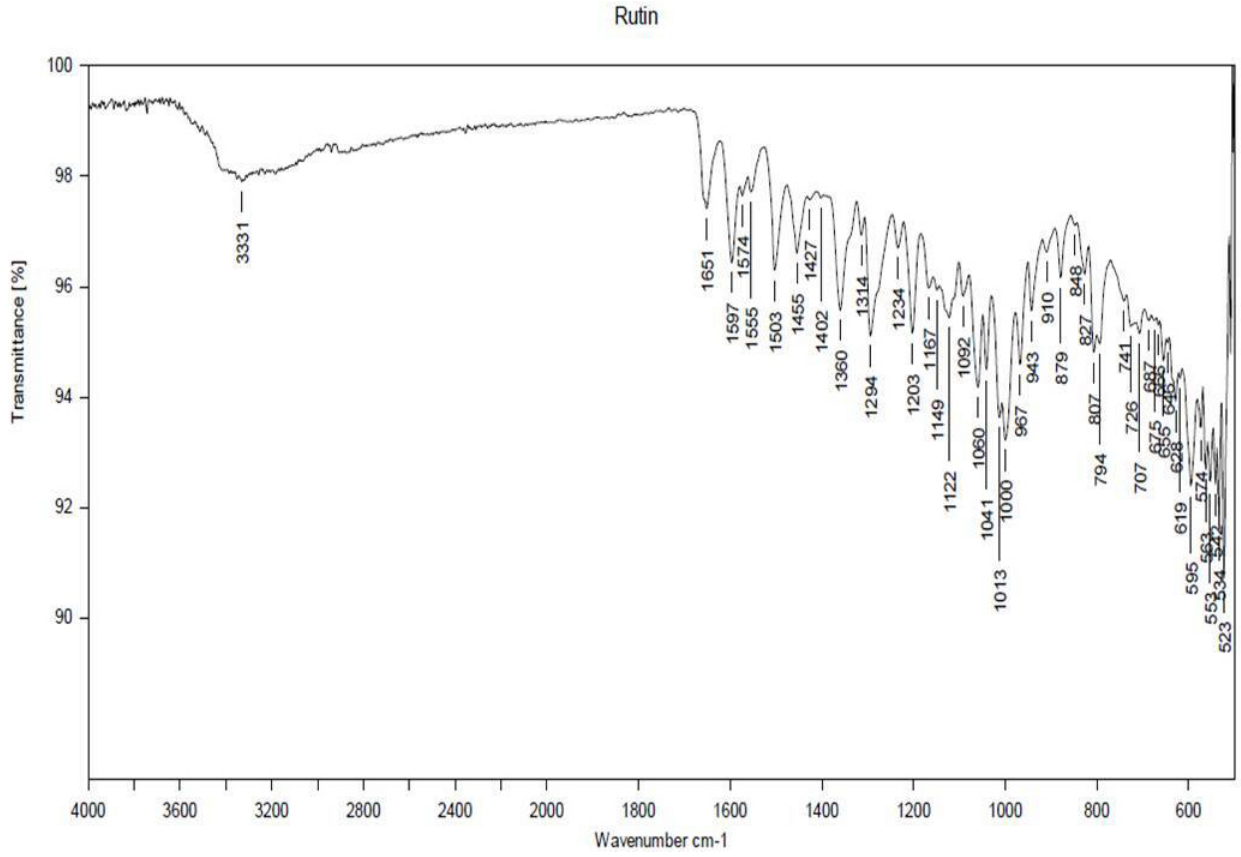

Fig. 2. Fourier transform-infrared (FT-IR) spectroscopy of Rutin.

ration by heating to obtain drug-loaded in mesoporous silica material. As observed in previous studies, the solvent evaporation method gives the drug molecules enough time to rearrange and aggregate inside the mesopores [22–24].

Powder X-Ray Diffraction

The pore structure of the materials was characterized using X-ray diffraction analysis on a Bruker D2 Phaser device (Model: 995411, Bruker Inc, Malvern, PA, USA). CuK radiation (k = 1.54 Å) with a Ni filter was employed for the analysis. The measurement involved a step size of 0.01° and utilized divergent slots and a convergent slit width of 0.1 mm and 3 mm, respectively. The X-ray diffraction experiment was conducted with a 10 mA current and a 30 kV voltage, while a LYNXEYE detector (Model: B08421, Bruker Inc, Malvern, PA, USA) was used to capture the diffraction patterns [25].

Scanning Electron Microscopy and Particle Size Distribution

The morphology and particle size of pure Rutin, SBA-15, and Rutin-loaded silica was observed through scanning electron microscopy (Instrument ID # 0014785, *SEM*, VEGA II LSH, TESCAN, Czech Republic). Before stan-

Journal of
BIOLOGICAL REGULATORS
and Homeostatic Agents

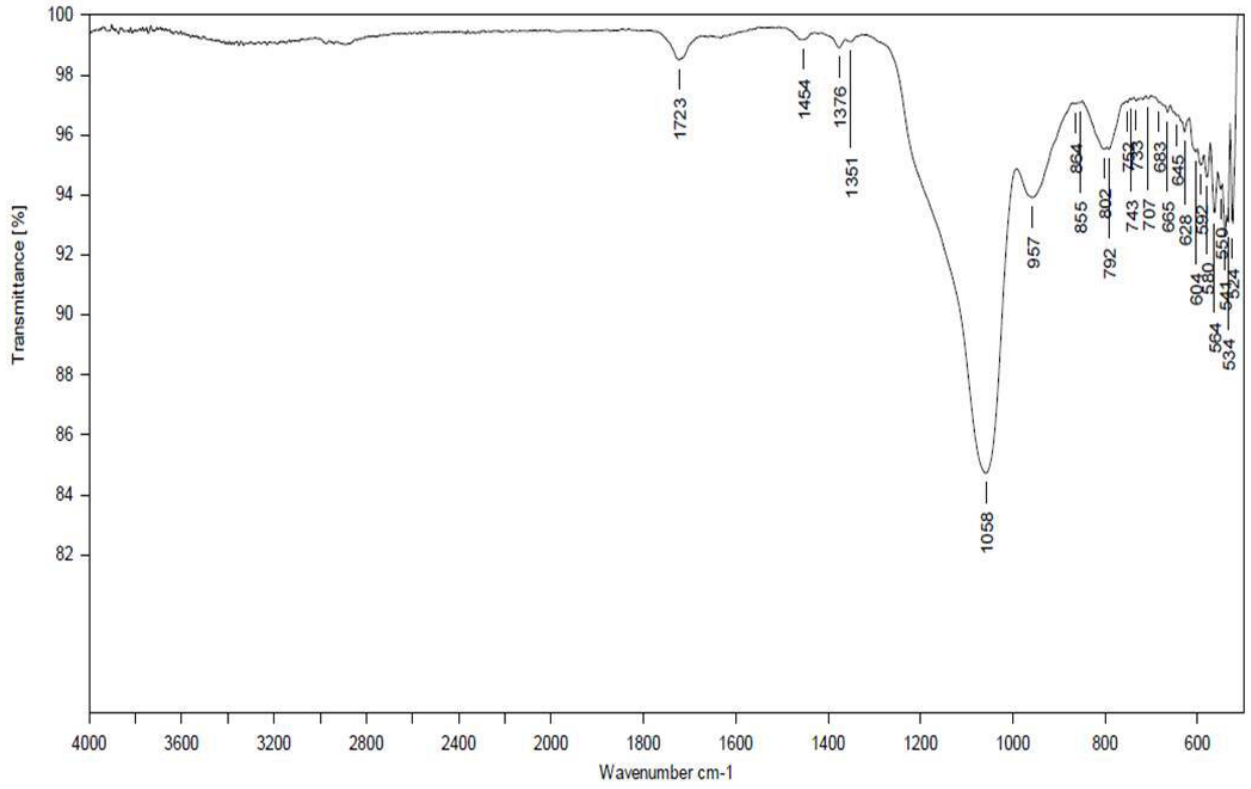

Fig. 3. Fourier-transform infrared spectroscopy of mesoporous SBA-15.

dard error of the mean (SEM) imaging, samples were coated with gold by a sputter coater. Approximately 1 mg of each sample was placed onto a double-sided adhesive strip on a sample holder [26].

Fourier Transform-Infrared (FT-IR) Spectroscopy

The chemical identity of pure materials (SBA-15, Rutin, Batch number: 01462M, HiMedia Laboratories, Mumbai, India) and the loaded ones (Rutin/SBA-15) was verified by diffuse reflectance infrared Fourier transform spectroscopy (DRIFTS, Nicolet 6700 FT-IR spectrometer, Model: 987436, Thermo Fisher Scientific, Waltham, MA, USA). The samples were mixed with KBr and the IR spectra were obtained between 400 and 4000 cm^{-1} [27].

Differential Scanning Calorimetry

Differential scanning calorimetry (DSC, TA Instruments, Model: 98114, New Castle, DE, USA) is a thermal analysis technique used to study the thermal behavior of materials, including drug-loaded mesoporous materials. DSC measures the heat flow as a function of temperature or time, and it is commonly used to investigate changes in the physical and chemical properties of materials during thermal processing, such as melting, crystallization, and phase transitions. When drug molecules are loaded into mesoporous materials, the DSC thermogram of the drug-loaded mesoporous material can provide valuable information about the interaction between the drug molecules and the host mesoporous material [28].

Solubility Studies

Solubility measurements were performed in various solvents such as water, 1.2 pH buffer, and 6.8 pH phosphate buffer at room temperature. The equivalent weight of 100 mg Rutin was added to 100 mL solvent. The samples were subjected to constant shaking for 6 h with a magnetic stirrer then filtered (0.22 micron), diluted, and analyzed by UV-VIS spectrophotometer (Model # 35563, Cole-Parmer Ind Ltd., Mumbai, India) at 360 nm. The same procedure was repeated for various formulations [29].

Estimation of Percent Yield

The percent yield of the formulation was calculated by considering the total amount of the obtained product. Theoretical weight was calculated while considering the weight of the drug and polymers employed during the preparation [30].

The percent yield was calculated by using as following equation:

$$\text{Percentage yield} = \frac{\text{weight of final formulation}}{\text{weight of drug} + \text{weight of mesoporous SBA-15}} \times 10$$

Determination of the Drug Loading Efficiency

The drug-loaded efficiency (EE) was calculated after extracting the drug from the prepared inclusion complex. Equivalent to 100 mg Rutin from the final product was in-

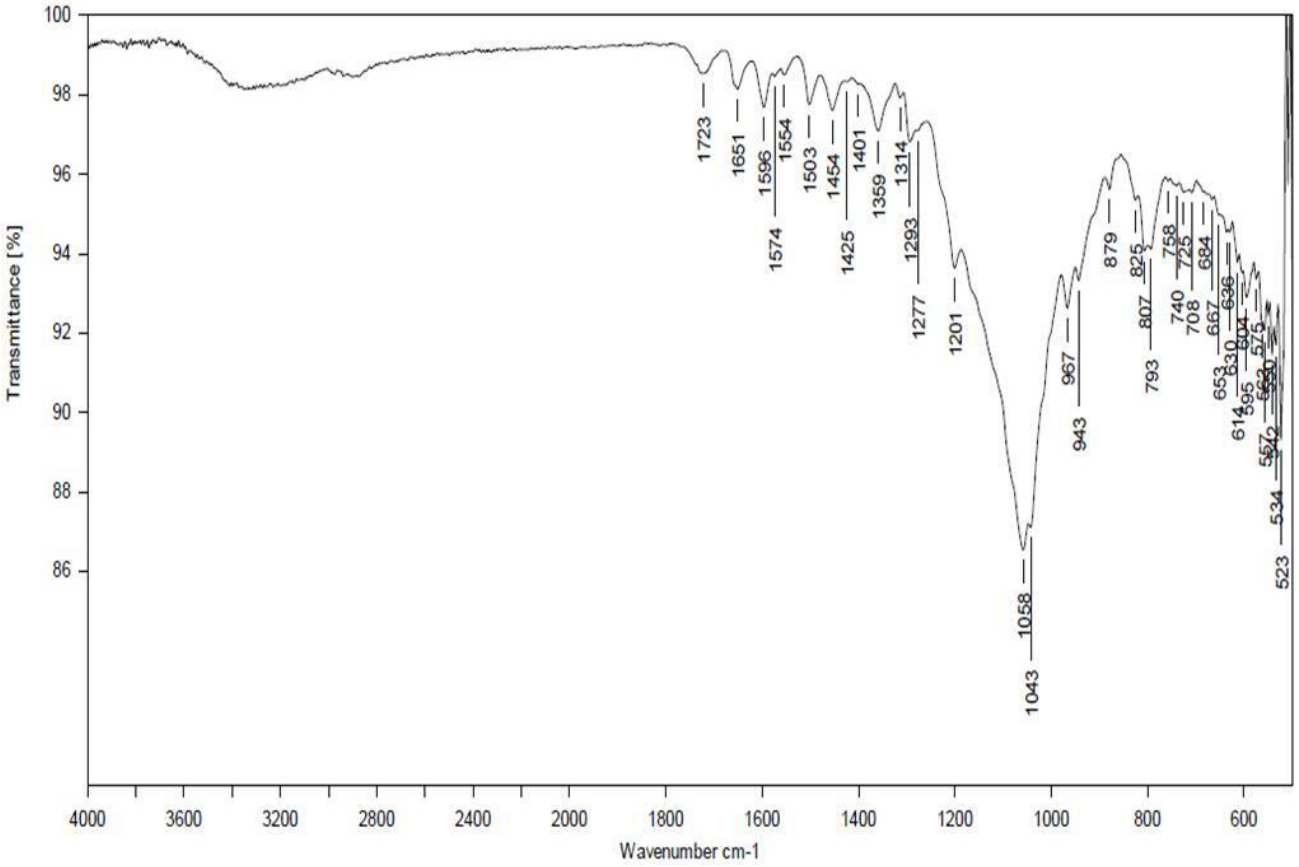

Fig. 4. Fourier-transorm infrared spectroscopy of Rutin and mesoporous SBA-15.

sulated in 100 mL of phosphate buffer (pH 6.8) and stirred magnetically at 500 rpm for 6 h for completely extracted Rutin. After completion of 6 h, these solutions were diluted and analyzed by a UV-VIS spectrophotometer (Model # 35563, Cole-Parmer Ind Ltd., Mumbai, India) at 360 nm. All trails were done in triplets. The percentage of drug-loaded was calculated by using the below equation [30]:

$$\text{Drug loaded } (\%) = \frac{\text{Practical drug loading}}{\text{Theoretical drug loading}} \times 100$$

Dissolution Rate of Rutin from SBA-15

The rate of dissolution of Rutin from SBA-15 in comparison to pure Rutin was assessed using dissolution apparatus I. A volume of 900 mL of HCl 0.1 N (pH 1.2) for 2 h and replaced by phosphate buffer (6.8 pH) for 7 h was used as a dissolution medium at 37 °C with a speed of 100 rpm. About 100 mg of pure Rutin and equivalent to 100 mg of Rutin complex were packed in a muslin cloth and placed in each dissolution basket. The samples of 5 mL were taken every 1 h interval and to maintain a constant volume fresh medium was added (at 37 °C). The Rutin concentration was measured with a UV-VIS spectrophotometer (Model # 35563, Cole-Parmer India Ltd., Mumbai, India) at 360 nm. The assays were done in triplicate and mean values were calculated [28].

In-Vitro Drug Release Kinetics

The release kinetics of Rutin from different formulations were analyzed using various mathematical models to understand the mechanism of drug release. The following models were applied by using dissolution data (DD) Solver software (version 2.0, Excel add-in software package developed by QAT Software Development Services, Costa Rica, Brazil): zero-order kinetics, first-order kinetics, Hixson-Crowell kinetics, Higuchi's model, Korsmeyer-Peppas model, and Weibull model. Zero-order release kinetics refers to a constant drug release rate from a drug delivery device. It assumes that the release rate was independent of the drug concentration. First-order release kinetics describes drug release from a system where the release rate depends on the drug concentration. Hixson and Crowell observed that the surface area of particles is proportional to the cube root of their volume. Higuchi developed mathematical models to study drug release from insoluble matrices based on Fickian diffusion. The Korsmeyer-Peppas model describes the fractional drug release as exponentially related to the release time. It applies to polymeric systems such as slabs, cylinders, and spheres. The Weibull model is an empirical model widely used for different dosage formulations [31].

Journal of
BIOLOGICAL REGULATORS
and Homeostatic Agents

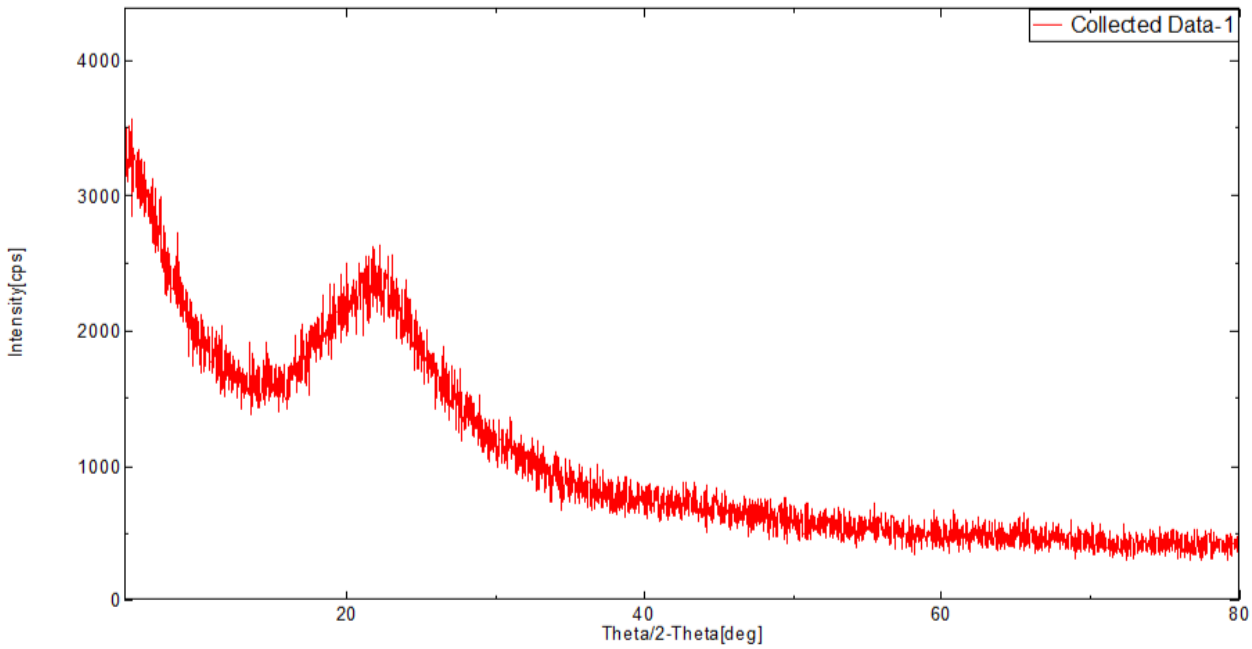

Fig. 5. Powder X-ray diffraction of formulation with ethanol 3 (FE3).

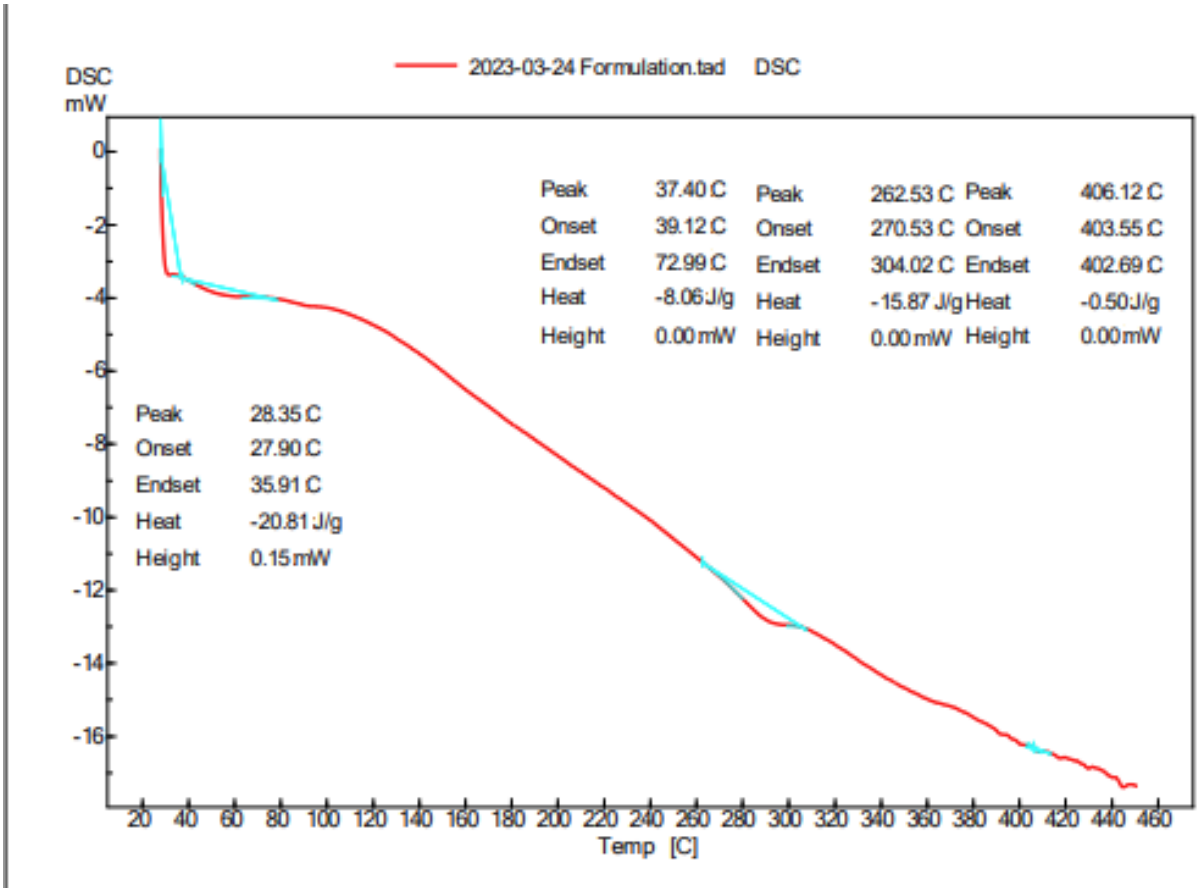

Fig. 6. DSC analysis of formulation FE3 depicts endothermic peaks corresponding to its melting points, with peak positions into its thermal stability. DSC, differential scanning calorimetry.

Statistics

The data obtained from the current study was subjected to statistical analysis by one way analysis of variance (ANOVA) followed by Dunnett's Multiple Comparison Test to evaluate the significant variation from best formulation (formulation with ethanol 3 (FE3)). *p* value less than 0.05 was considered to indicate the significance level upon comparison.

Results

Characterization of Rutin/SBA-15 Complex

Fourier Transform-Infrared (FT-IR) Spectroscopy

Analysis of results from Figs. 2,3,4 suggested that O-H stretching vibration typically observed at 3200–3600 cm^{-1} is absent in Fig. 3 (SBA-15). However, such O-H stretching was observed in Rutin (Fig. 2) and Rutin/SBA-15 complex (Fig. 4). Furthermore, the analysis also indicated that C-O stretching vibration typically observed in the range of 1650–1800 cm^{-1}, was found in Fig. 2 (Rutin), Fig. 3 (SBA-15), and Fig. 4 (Rutin in SBA-15 polymer). The C-O stretching vibration for Rutin, Rutin + polymer occurred at 1651 cm^{-1}, while in mesoporous SBA-15 sample occurred at 1723 cm^{-1}. These figures suggested the presence of characteristic features including the functional groups of Rutin as well as SBA-15 in the formulation.

Powder X-Ray Diffraction

The X-ray diffraction analysis of different samples is indicated in Fig. 5. The important analysis of data suggested that the peak was slightly asymmetry with the asymmetry factor of 1.01188. The Lorentz polarization factors for the low-angle and high-angle components were found to be 0.7485 and 0.0590474, respectively. Further, the estimated crystal size was 0.158636 Angstroms, with an estimated error of 0.1387 Angstroms. These values reflect the ideal size of the crystalline nature of the test compound in the formulation.

Differential Scanning Calorimetry

The differential scanning calorimetry (DSC) data of the Rutin/SBA-15 complex is summarized in Fig. 6. The DSC thermogram shows the thermal behavior of formulation formulation with ethanol 3 (FE3). Peak observed at 262.53 °C, corresponds to the drug component within formulation FE3, indicating a specific thermal event associated with the drug substance. This peak is essential for assessing the thermal behavior and stability of the drug within the formulation.

Additionally, other peaks observed in the thermogram correspond to thermal events associated with the mesoporous silica component present in formulation FE3. These peaks provide insights into the thermal behavior of the mesoporous silica material under the tested conditions.

However, the analysis also indicates the absence of a melting peak within the different temperature ranges, signifying the non-deteriorating property of the formulation. This absence of a melting peak, combined with the specific peak corresponding to the drug and the observed peaks related to mesoporous silica, underscores the formulation's remarkable thermal stability under the tested conditions.

Scanning Electron Microscopy (*SEM*)

The scanning electron microscopy (*SEM*) images obtained for the Rutin/SBA-15 complex are indicated in Fig. 7. The analysis of the images provided information about the shape and distribution of various mesoporous particles. Further, the pore structure of the samples can be observed in the images of the mesoporous complex. The micrographs of *SEM* indicated that the particle size of Rutin/SBA-15 polymer has an approximate size of 10 µm.

Determination of Solubility

The prepared Rutin mesoporous complex solubility was determined by using various solvents like water, pH 1.2 acidic buffer (Batch number: 00975, HiMedia Laboratories, Mumbai, India, and 6.8 phosphate buffer (Batch number: 92547, HiMedia Laboratories, Mumbai, India) and reported in Table 1.

The solubility testing data for different samples using various solvents is represented in Table 2. Rutin was found to possess the lowest solubility value in water (0.087 mg/mL), pH 1.2 buffer (0.026 mg/mL), and pH 6.8 buffer (0.146 mg/mL). Among the different formulations tested, formulation with DMSO solvent 3 (FD3) was found to possess the lowest value in water (0.142 mg/mL), while FD2 was lowest in pH 1.2 buffer (0.032 mg/mL) and FD1 in pH 6.8 buffer (1.560 mg/mL). On the other hand, FE3 was found to exhibit the highest solubility values in all three tested solvents such as water (0.264 mg/mL), pH 1.2 buffer (0.190 mg/mL), and pH 6.8 buffer (2.514 mg/mL), suggesting that the formulation has perfect characteristics for oral administration.

Percentage Yield

The percentage yield was found to be in the range of 81% to 93.3%. Fig. 8 represents the percentage yields recorded for various formulations. Three different series of Rutin formulations such formulation with DMSO solvent (FD), formulation with ethanol (FE), formulation with methanol (FM) were tested. Maximum percentage yield was observed for FE series, among them FE3 was found to be the highest (93.3%), whereas FE2 and FE1 had 82% and 88% yield, respectively. In FD series, FD3 had the highest yield (91.6%) and both FD1 as well as FD2 had 84% yield. The lowest yield among all three series of formulations was recorded for FM1 (81.0%), while FM2 had 87.2% and FM3 had 86.2% yield. When compared, FE3 was more suitable for achieving the desired pharmacokinetic properties.

Journal of
BIOLOGICAL REGULATORS
and Homeostatic Agents

Table 2. Data for solubility determination.

SI. No	Formulation code	Water (mg/mL)	pH 1.2 buffer (mg/mL)	pH 6.8 buffer (mg/mL)
1.	Rutin	0.087 ± 0.02	0.026 ± 0.82	0.146 ± 0.04
2.	FD1	0.273 ± 0.01	0.034 ± 0.03	1.560 ± 0.12
3.	FD2	0.269 ± 0.05	0.032 ± 0.09	1.700 ± 0.08
4.	FD3	0.142 ± 0.06	0.051 ± 0.06	1.802 ± 0.14
5.	FE1	0.228 ± 0.01	0.099 ± 0.12	2.410 ± 0.02
6.	FE2	0.245 ± 0.02	0.111 ± 0.10	2.486 ± 0.02
7.	FE3	0.264 ± 0.01	0.190 ± 0.85	2.514 ± 0.06
8.	FM1	0.224 ± 0.12	0.062 ± 0.16	2.201 ± 0.10
9.	FM2	0.202 ± 0.08	0.066 ± 0.04	2.248 ± 0.14
10.	FM3	0.223 ± 0.12	0.087 ± 0.03	2.257 ± 0.09

Data are expressed as Mean ± SD (n = 3). SD, standard deviation.

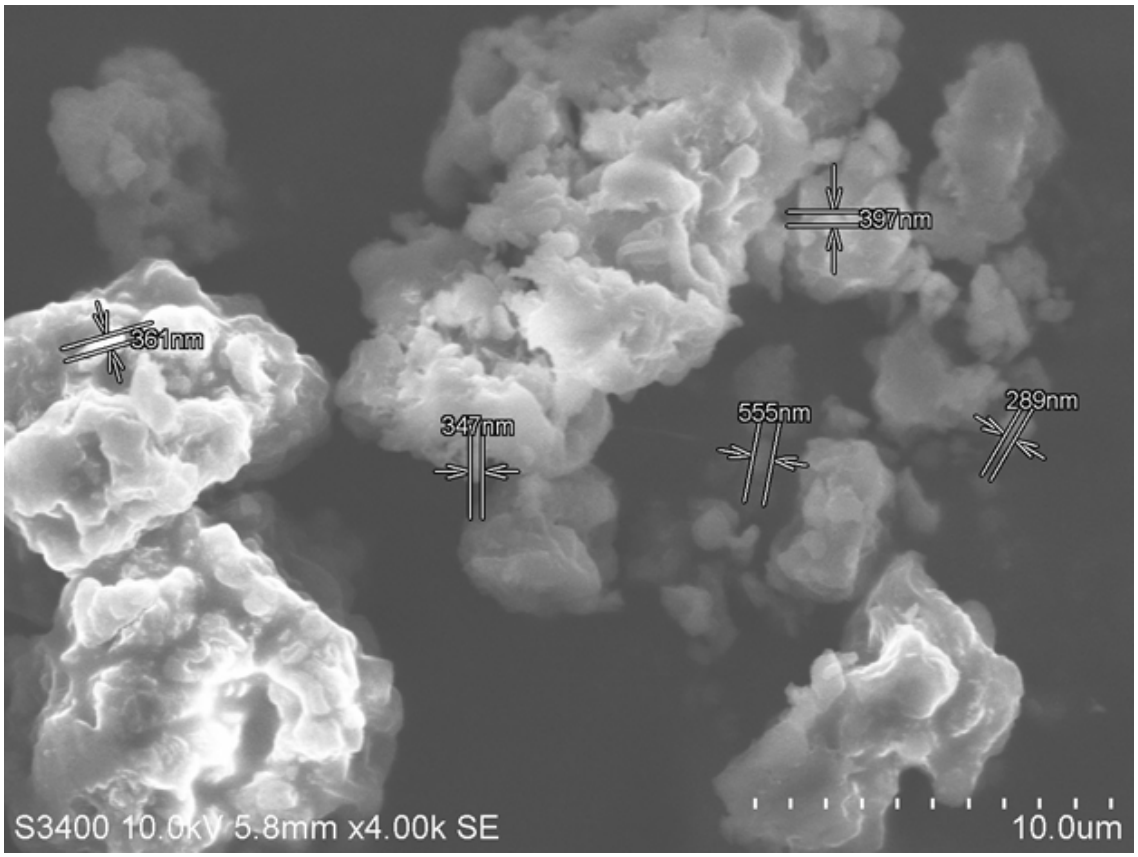

Fig. 7. Scanning electron microscopy images of mesoporous silica material (SBA-15) with Rutin in the formulation. The distance between the two arrows indicates the porous size of SBA-15. SE, scanning electron; um, µm.

Drug Loading Efficiency

The percentage of drug loading efficiency of all the formulations was in the range of 68.2% to 71.2%. The percentage drug entrapment efficiency of the prepared Rutin-mesoporous SBA-15 complex is shown in Fig. 9. Three different series of formulation such as FD, FE and FM were tested in the present study. In comparison to the other formulations, the FE series formulations have a usually greater drug loading efficacy, ranging from 70.1% to 71.2%, suggesting better drug encapsulation. The drug encapsulation efficacies of FD1, FD2, FD3, FM1, FM2, and FM3 range from 67.3% to 69.4% and 68.2% to 68.8%, respectively, indicating reduced drug encapsulation efficiency when compared to the FE series.

In-Vitro Dissolution Study

The data from Fig. 10 indicates that the percentage of drug release varies among different formulations. Rutin shows a gradual increase in drug release, reaching 35.92% at 9 hours. FD1, FD2, and FD3 start with higher initial drug release percentages but have slower release rates. FE1 releases a large amount of the medication at first, then drops

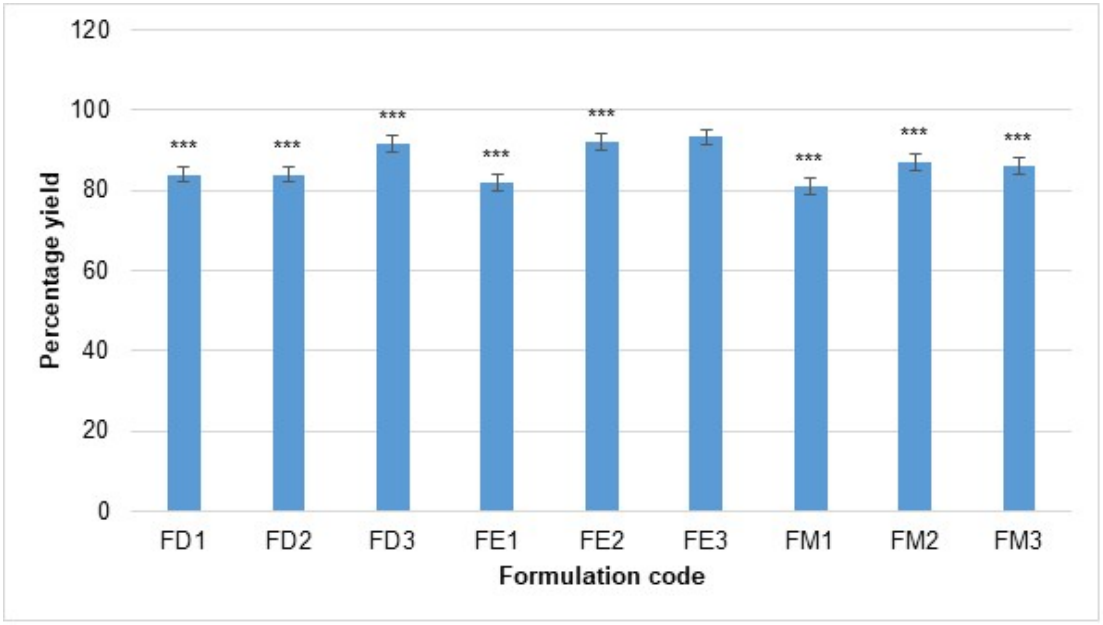

Fig. 8. Percentage yield of Rutin-mesoporous SBA-15 complex. Significant at ***$p < 0.001$; Values are Mean ± SD (n = 3); one way analysis of variance (ANOVA) followed by "Dunnett's Multiple Comparison Test" where data was compared with the Best formulation FE3 (control).

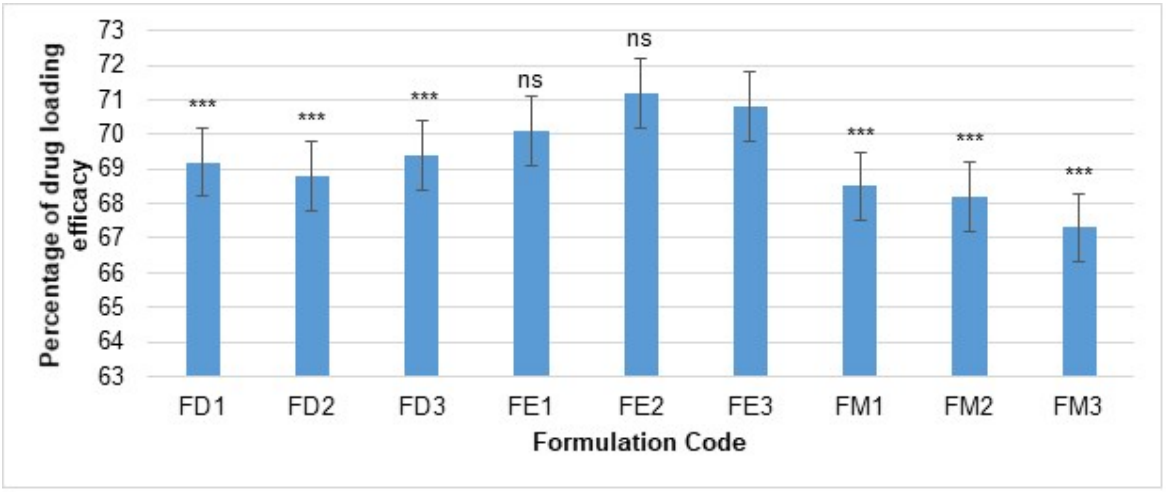

Fig. 9. Percentage of Drug loading efficacy of Rutin-mesoporous SBA-15 complex. Significant at ***$p < 0.001$; ns, no significant. Values are Mean ± SD (n = 3); one way analysis of variance (ANOVA) followed by "Dunnett's Multiple Comparison Test" where data were compared with the Best formulation FE3 (control).

off a little bit before continuing to release the drug until 9 hours later, when it reaches 66.13%. FE2 releases at a lower beginning rate but grows quickly, reaching 72.58% after 9 hours. FE3 has a similar starting point as FE2 but has a slower release rate, releasing 83.83% at 9 hours. FM1, FM2, and FM3 start with lower initial releases but steadily increase, with FM3 reaching 68.64% at 9 hours. The ideal release characteristics can be observed with FE3 formulation.

Kinetic Drug Release Study of Formulation FE3 from DD Solver Software

As shown in Table 3, among the various kinetics models evaluated for formulation FE3, the zero-order and first-order models showed high R-squared values (0.9549 and 0.9644, respectively) and low mean square error (MSE) values, indicating a good fit to the data. The Higuchi model seems to fit less well, as seen by its higher MSE value and lower R-squared value of 0.8840. The Korsmeyer-Peppas, Hixson-Crowell, and Hopfenberg models, on the other hand, showed low MSE values and high R-squared

Journal of
BIOLOGICAL REGULATORS
and Homeostatic Agents

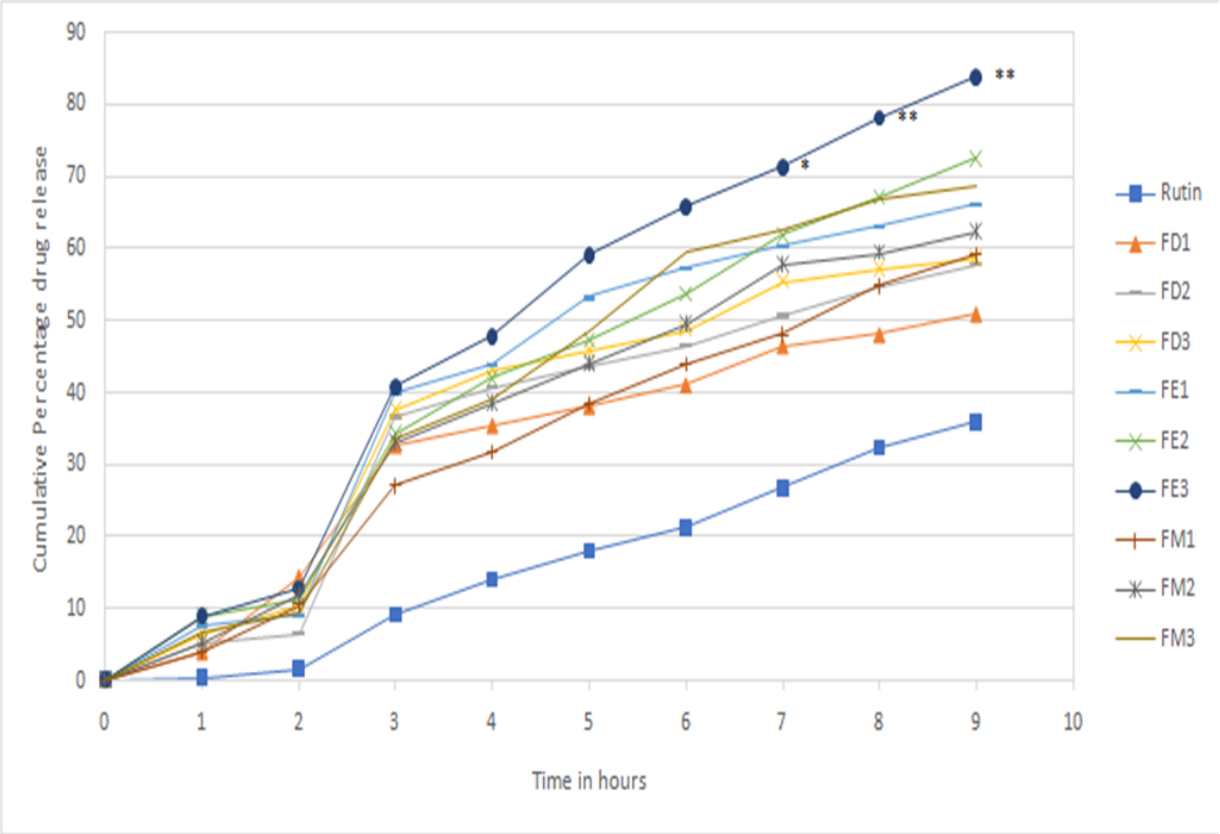

Fig. 10. ***In-vitro*** **drug release study of Rutin and prepared formulation.** Significant at $*p < 0.01$; $**p < 0.001$; Values are Mean ± SD (n = 3); one way analysis of variance (ANOVA) followed by Dunnett's Multiple Comparison Test. Values were compared for formulation with control Rutin.

values (0.9668, 0.9719, and 0.9757, respectively), indicating good fits. The Baker-Lonsdale model had a lower R-squared value (0.8337) and a higher MSE value, indicating a weaker fit. Finally, the Weibull model showed the highest R-squared value (0.9859) and lowest MSE value, indicating the best fit to the data. These factors indicated the kind of matrix that makes up a formulation, as well as its drug elimination and releasing properties.

Discussion

In the present study, different formulations of mesoporous SBA-15 with Rutin were tested. The results suggested that the FE3 formulation exhibited the characteristics of Rutin being embedded in mesoporous SBA-15 polymer. The compound had the necessary physical characteristics for ideal dissolution and was thermally stable. The solubility analysis also showed that the FE3 formulation had the best loading efficiency, best dissolving in a range of pH-varying solvents, and best releasing properties. Further, the kinetic properties of FE3 can be explained by the Weibull model, suggesting the suitability of the formulation for oral administration (Figs. 2,3,4,5,6,7,8,9,10 and Table 2).

Fourier transform-infrared (FT-IR) spectroscopy is known to be a valuable technique for evaluating the compatibility between drugs and polymers. According to the literature, the O-H stretching vibration, typically observed in the range of 3200–3600 cm^{-1}, was found to be absent in the mesoporous sample, indicating the absence of the O-H functional group [32]. On the other hand, both the drug with polymer sample and the Rutin sample exhibit an O-H stretching vibration at 3300 cm^{-1} and 3331 cm^{-1}, respectively. This suggested that the drug complexes with the SBA-15 [32].

In addition, the FT-IR analysis also suggested the presence of a C-O functional group. Study conducted in the past suggested that C-O stretching vibration can be found in the range of 1650–1800 cm^{-1} [32]. The present study data indicated that the C-O stretching occurred in all three samples. The findings are by previous results where the presence of carbonyl group is reported in both Rutin as well in SBA-15 [27]. Furthermore, the comparison of values of the O-H stretching vibration (3331 cm^{-1} for Rutin) and the C-O stretching vibration (1360 cm^{-1}) between the mesoporous and Rutin samples showed similarities. These similarities suggest the possibility of compatibility between mesoporous and Rutin for formulation purposes [32].

The split pseudo-Voigt function is suggested by the peak form seen in X-ray diffraction experiments, as docu-

Table 3. Kinetic drug release study of FE3 from dissolution data (DD) Solver goodness of fit parameters.

Model & Equation	Goodness of fit parameters						
	R_obs-pre	Rsqr	MSE	MSE_root	SS	AIC	MSC
Zero-order F = k0 × t	0.9785	0.9549	41.5427	6.4454	373.884	61.2395	2.5910
First-order F = 100 × [1 – Exp(– k1 × t)]	0.9873	0.9644	32.7841	5.7257	295.056	58.8717	2.8277
Higuchi F = kH × t ^ 0.5	0.9615	0.8840	106.7551	10.3322	960.796	70.6776	1.6471
Korsmeyer-Peppas F=kKP × t ^ n	0.9837	0.9668	34.3827	5.8637	275.061	60.1700	2.6979
Hixson-Crowell F=100 × [1 – (1 – KHC × t) ^ 3]	0.9891	0.9719	25.8699	5.0862	232.828	56.5030	3.0646
Hopfenberg F=100 × [1 – (1 – KHB × t) ^ n]	0.9887	0.9757	25.1239	5.0124	200.991	57.0326	3.0116
Baker-Lonsdale 3/2 × [1 – (1 – F/100) ^ (2/3)] – F/100 = kBL × t	0.9414	0.8337	153.0887	12.3729	1377.798	74.2824	1.2867
Weibull F = 100 × {1 – Exp [– ((t – Ti) ^ β)/α]}	0.9929	0.9859	16.6794	4.0840	116.755	53.6008	3.3548

MSE, mean square error; SS, sum of squares; AIC, akaike information criterion; MSC, model selection criterion; KHC, Hixson-Crowell constant.

mented in the literature. This peak illustrates the disordered pore configurations and amorphous characteristics that are typically observed in mesoporous materials [25]. Besides, the peak shape, d-spacing value, peak intensity, and the presence of a broad peak are consistent with the amorphous nature and disordered structure of mesoporous materials [29]. Considering the characteristics of mesoporous materials, such as their high surface area, large pore volume, and narrow pore size distribution, the obtained X-ray diffraction values align with those expected for mesoporous materials [31].

Furthermore, the asymmetry peak observed with the X-ray diffraction study could be related to several causes such as operational procedure, equipment handling as well as sample tested. As reported in literature, a slight variation in asymmetry peak is acceptable and can be adjusted through the operational method of the instrument and need not necessarily suggests the sample deterioration [33]. Lorentz polarization factor in X-ray diffraction analysis suggests the geometry of the sample and single/polycrystal size in the irradiation of crystalline sample powder. When compared with previous study, the Lorentz polarization values for the tested formulations in the present study are within the suitable range [34]. The study suggested that such crystalline nature of the compound is essential for optimum efficacy [31]. In addition, the crystals of the formulations have ideal size, and such characteristics according to earlier study is preferred in the new drug delivery system for reaching the desired area of the body [35].

A study conducted in the past suggests that DSC provides vital information about various thermal events, including the onset temperature, peak temperature, end set temperature, heat flow, and height [28]. From the observations of the present study, it can be indicated that the Rutin-mesoporous possesses an amorphous structure and complex is thermally stable up to 262 °C [36]. Important details about the size, shape, pore structure, and distribution of the mesoporous particles were revealed by the *SEM* images shown in Fig. 7. According to earlier research, mesoporous materials often have a large surface area and a noticeable level of porosity; these characteristics can be seen and measured via *SEM* analysis [37]. Moreover, *SEM* analysis is reported to provide information about the determination of particle size distribution. Besides, by measuring the sizes of multiple particles in the *SEM* images, it is possible to calculate the average particle size and assess the size distribution [38]. The *SEM* micrograph analysis in the present study reveals particles with an approximate size of 10 µm.

The solubility study suggests that the FE3 formulation has more solubility values than others, including pure Rutin, in all tested solvents. As recorded in previous research, the solubility factor of a formulation plays a vital role in achieving the desired concentration in biological fluids. As reported in the literature, the solubility of a formulation is generally tested in a range of solvents having different degrees of pH values [39]. Such type of study provides information about the dissolution characteristics of the formulation in an acidic and basic atmosphere of the stomach and intestine, respectively [40]. A drug having anticipated solubility in solvents of different pH is reported to achieve satisfactory therapeutic concentration after oral administration [41]. This enhancement in solubility can be at-

Journal of
BIOLOGICAL REGULATORS
and Homeostatic Agents

tributed to the porous structure of the mesoporous materials, which hinders the formation of crystalline Rutin and stabilizes the drug molecules in an amorphous state [37]. As reported in the literature, unlike crystalline solids, amorphous solids have lower packing energy and lack long-range order in molecular packing, leading to improved solubility compared to their crystalline counterparts [42]. DSC analysis further confirmed the amorphous state of the Rutin/SBA-15 complex. The abundant pore volume in the mesoporous materials facilitated better drug penetration, promoting increased contact with the surrounding medium and consequently enhancing the drug's solubility [43].

The percentage yield study suggested that FE series formulations demonstrate higher efficiency in converting starting materials to the desired product, while the FM series shows lower efficiency. Previous research has suggested that drug yield and loading efficiency play an important part and are considered a challenging task in targeted drug delivery systems. These physical parameters establish the accommodative ability of the carriers towards the test drug in a formulation [43]. The better efficacy could be related to the molecular distribution and particle size of the Rutin/SBA-15 complex [41,43]. Similarly, the loading efficacy was also observed to be better for FE formulations compared to others. Factors such as drug properties, formulation composition, and processing conditions could influence drug loading efficacy [44]. As indicated in previous study, higher drug loading efficacy is desirable for increased drug concentration at the target tissue, potentially improving drug efficacy [45]. Moreover, formulations having higher yield and loading capacity have shown better therapeutic interventions when tested in several clinical diseases [41,44].

The dissolution study data suggested that the formulations exhibit different release rates and percentages overtime periods. Among the different formulations, FE3 although has a lower initial release achieved approximately 83.83% of the drug release within 9 hours. In comparison, pure Rutin showed a drug release of about 35.92% during the same period. According to the literature, the higher dissolution rate in the FE3 formulation could be attributed to the adsorption branch, chosen due to the cage-like pore structure facilitating percolation phenomena during the desorption branch [46,47].

In this study, *in-vitro* drug release data was analyzed using various kinetics models, including zero-order, first-order, Higuchi, Korsmeyer-Peppas, Hixson-Crowell, Bakar-Lonsdale, Hopfenberg, and Weibull. The dissolution data (DD) Solver software provided several statistical criteria for evaluating the dissolution models, such as R2 adjusted, akaike information criterion (AIC), and model selection criterion (MSC) [48]. After calculating each model's goodness of fit parameters, the model with the highest MSC value was deemed to be the best [49].

The zero-order model assumes a constant drug release rate, while the first-order model assumes a rate proportional to the remaining drug amount [50]. Moreover, the kinetic drug release study revealed that all formulations were fitted to different models such as zero-order, first-order, Higuchi, Korsmeyer-Peppas, Hixson-Crowell, Hopfenberg, Baker-Lonsdale, and Weibull [51]. The R-squared values fell within the acceptable range for all formulations [52]. However, FE3 demonstrated the highest K0 value, indicating the fastest rate of drug release among all formulations. Additionally, the n value for FE3 was 0.845, suggesting a non-Fickian (anomalous) diffusion mechanism. The Hixson-Crowell constant (KHC) value was also higher for FE3 compared to other formulations, indicating a higher drug release [53]. The data suggested that the drug in the formulation is eliminated at constant rate as well depending on plasma concentration. Besides, the drug was observed to be soluble and released from the formulation as indicated from values of Higuchi and Korsmeyer-Peppas models. The Hixson-Crowell model predicted the precise mechanism of drug release from formulation [54]. The optimum release phenomenon of the drug from polymer such as SBA-15 and its degradation properties was found to be satisfactory from Hopfenberg study. The desired controlled/sustained released parameter of Rutin from spherical matrix of formulation was observed with Baker-Lonsdale model [55]. The Weibull model suggested the distribution as well as decomposition of the drug in formulation and the values were indicative of reasonable for formulation, when compared with previous study [56].

Overall, the analysis suggests that FE3 is the ideal formulation, and the drug release could be controlled through the diffusion process [57]. Besides, FE3 has the highest solubility, indicating that the concentration of mesoporous SBA-15 increases the solubility and a higher rate of solubility can be advantageous in certain applications, such as drug delivery, where rapid release of the active compound is desired [58,59]. The appropriate characteristics observed in the FE3 formulation could be linked to the ethanol being used as a solvent while preparing the mesoporous particles of Rutin since ethanol can dissolve a wide range of polar and non-polar substances [60]. However, the role of SBA-15 on influencing the release of Rutin in other experimental setup including the *in-vivo* studies needs to be evaluated.

Conclusion

The synthesized SBA-15 with Rutin exhibited optimum physico-chemical characteristics, without undergoing any self-modification or interference with drug's nature. The kinetics data suggested that Rutin has improved oral bioavailability with SBA-15 that might be suitable for targeted drug delivery system. The technique of formulating SBA-15 with Rutin is simple and can solve the major issue of poor solubility/distribution associated with Rutin.

This might enhance the scope of utilizing Rutin for treating various illnesses. However, more research is necessary to evaluate the *in-vivo* pharmacokinetic performance of Rutin/SBA-15 and its suitability for various pharmacological activities.

Availability of Data and Materials

The datasets used and/or analyzed during the current study are available from the corresponding authors upon reasonable request.

Author Contributions

SFR, SA, KD and SV designed the research study. SA, AMSK, MEMA, FA, SIR and SMBA carried out the experimental part of the research. SFR, FA, SIR and SMBA provided help and advice on research methodology and analysis of data. KD, MEMA and FA analyzed the data. AMSK, SA and KD wrote the manuscript. SIR and SMBA edited and reviewed the manuscript. All authors contributed to editorial changes in the manuscript. All authors read and approved the final manuscript. All authors have participated sufficiently in the work and agreed to be accountable for all aspects of the work.

Ethics Approval and Consent to Participate

Not applicable.

Acknowledgment

The authors are thankful to Mallige College of Pharmacy, Bangalore, for generously providing the necessary facilities and chemicals for the compilation of research work. The authors would also like to acknowledge the financial support offered by King Saud University Researchers Supporting Project number RSP2024R146. The authors also thank AlMaarefa University, Riyadh, Saudi Arabia, for extending financial support for this research.

Funding

This research was funded by the Researchers Supporting Project number (RSP2024R146) at King Saud University, Riyadh, Saudi Arabia.

Conflict of Interest

The authors declare no conflict of interest.

References

[1] Patel K, Patel DK. The beneficial role of rutin, a naturally occurring flavonoid in health promotion and disease prevention: A systematic review and update. Bioactive food as dietary interventions for arthritis and related inflammatory diseases. Academic Press. 2019; 457–479.

[2] Frutos MJ, Rincón-Frutos L, Valero-Cases E. Rutin. In Nonvitamin and nonmineral nutritional supplements (pp. 111–117). Academic Press: Elsevier, Amsterdam. 2019.

[3] Riaz H, Raza SA, Aslam MS, Ahmad MS, Ahmad MA, Maria P. An Updated Review of Pharmacological, Standardization Methods, and Formulation Development of Rutin. Journal of Pure and Applied Microbiology. 2018; 12: 127–132.

[4] Başaran E, Öztürk AA, Şenel B, Demirel M, Sarica Ş. Quercetin, Rutin And Quercetin-Rutin Incorporated Hydroxypropyl β-Cyclodextrin Inclusion Complexes. European Journal of Pharmaceutical Sciences. 2022; 172: 106153.

[5] Ozturk AA, Basaran E, Senel B, Demirel M, Sarıca S. Synthesis, characterization, antioxidant activity of Quercetin, Rutin and Quercetin-Rutin incorporated β-cyclodextrin inclusion complexes and determination of their activity in NIH-3T3, MDA-MB-231 and A549 cell lines. Journal of Molecular Structures. 2023; 1282: 135169.

[6] Nguyen VK, Ta TT, Hoang AT. Preparation of solid dispersion of rutin by spay drying. VNU Journal of Science: Medical and Pharmaceutical Sciences. 2019; 35.

[7] Naeem A, Yu C, Zang Z, Zhu W, Deng X, Guan Y. Synthesis and Evaluation of Rutin-Hydroxypropyl β-Cyclodextrin Inclusion Complexes Embedded in Xanthan Gum-Based (HPMC-*g*-AMPS) Hydrogels for Oral Controlled Drug Delivery. Antioxidants. 2023; 12: 552.

[8] Liu J, Zhang S, Zhao X, Lu Y, Song M, Wu S. Molecular simulation and experimental study on the inclusion of rutin with β-cyclodextrin and its derivative. Journal of Molecular Structures. 2022; 1254: 132359.

[9] Franco P, De Marco I. Formation of Rutin-β-Cyclodextrin Inclusion Complexes by Supercritical Antisolvent Precipitation. Polymers. 2021; 13: 246.

[10] Kamel R, Basha M. Preparation and in vitro evaluation of rutin nanostructured liquisolid delivery system. Bulletin of Faculty of Pharmacy. 2013; 51: 261–272.

[11] Ismail A, El-Biyally E, Sakran W. An Innovative Approach for Formulation of Rutin Tablets Targeted for Colon Cancer Treatment. AAPS PharmSciTech. 2023; 24: 68.

[12] Kusuma MP, Sushmitha C. Design, formulation and optimization of rutin trihydrate emulgel by response surface methodology. International Journal of Pharmaceutical Sciences and Research. 2021; 11: 5799–5804.

[13] Abualhasan M, Assali M, Mahmoud A, Zaid AN, Malkieh N. Synthesis of Rutin Derivatives to Enhance Lipid Solubility and Development of Topical Formulation with a Validated Analytical Method. Current Drug Delivery. 2022; 19: 117–128.

[14] Saha S, Mishra A. A facile preparation of rutin nanoparticles and its effects on controlled growth and morphology of calcium oxalate crystals. Journal of Crystals Growth. 2020; 540: 125635.

[15] De Gaetano F, Cristiano MC, Venuti V, Crupi V, Majolino D, Paladini G, *et al*. Rutin-Loaded Solid Lipid Nanoparticles: Characterization and In Vitro Evaluation. Molecules. 2021; 26: 1039.

[16] Ahmed H, Gomte SS, Prathyusha E, Prabakaran A, Agrawal M, Alexander A. Biomedical applications of mesoporous silica nanoparticles as a drug delivery carrier. Journal of Drug Delivery Sciences and Technology. 2022; 76: 103729.

[17] Ravindran Girija A, Palaninathan V. Multifunctional Mesoporous Silica Nanoparticles for Biomedical Applications. Nano Medicine and Nano Safety. 2020; 10: 213–235.

[18] Ajiboye AL, Jacopin A, Mattern C, Nandi U, Hurt A, Trivedi V. Dissolution Improvement of Progesterone and Testosterone via Impregnation on Mesoporous Silica Using Supercritical Carbon Dioxide. AAPS PharmSciTech. 2022; 23: 302.

[19] Riikonen J, Xu W, Lehto VP. Mesoporous systems for poorly soluble drugs - recent trends. International Journal of Pharmaceutics. 2018; 536: 178–186.

[20] Zhao D, Feng J, Huo Q, Melosh N, Fredrickson G, Chmelka B, *et al*. Triblock copolymer syntheses of mesoporous silica with periodic 50 to 300 angstrom pores. Science. 1998; 279: 548–552.
[21] Belmoujahid Y, Bonne M, Scudeller Y, Schleich D, Grohens Y, Lebeau B. SBA-15 mesoporous silica as a super insulating material. European Physicists Journal of Specific Topics. 2015; 224: 1775–1785.
[22] Sheeba FR, Venkatesham A, JeyaAnanthi J. Mesoporous Santa Barbara Amorphous for Novel Drug Delivery System. International Journal of Pharmaceutical Sciences and Inventions. 2023; 12: 11–21.
[23] Tella JO, Adekoya JA, Ajanaku KO. Mesoporous silica nanocarriers as drug delivery systems for anti-tubercular agents: a review. Royal Society Open Science. 2022; 9: 220013.
[24] Alkahtani S, Alarifi S, Aljarba NH, Alghamdi HA, Alkahtane AA. Mesoporous SBA-15 Silica-Loaded Nano-formulation of Quercetin: A Probable Radio-Sensitizer for Lung Carcinoma. Dose Response. 2022; 20: 15593258211050532.
[25] Budiman A. Characterization of drugs encapsulated into mesoporous silica. International Journal of Applied Pharmacy. 2019; 11: 7–11.
[26] Qian H. Major Factors Influencing the Size Distribution Analysis of Cellulose Nanocrystals Imaged in Transmission Electron Microscopy. Polymers. 2021; 13: 3318.
[27] Paiva MRB, Andrade GF, Dourado LFN, Castro BFM, Fialho SL, Sousa EMB, *et al*. Surface functionalized mesoporous silica nanoparticles for intravitreal application of tacrolimus. Journal of Biomaterials Applications. 2021; 35: 1019–1033.
[28] Ahmad S, Javaid J, Fatima W. Controlled Release of Ibuprofen by Using Morphologically Modified Mesoporous Silica. Advances in Material Sciences and Engineering. 2022; 2022: 6376915.
[29] Li Q, Wang W, Hu G, Cui X, Sun D, Jin Z, *et al*. Evaluation of Chitosan Derivatives Modified Mesoporous Silica Nanoparticles as Delivery Carrier. Molecules. 2021; 26: 2490.
[30] Singh G, Sarwal A, Sharma S, Prasad P, Kuhad A, Ali W. Polymer-based prolonged-release nanoformulation of duloxetine: fabrication, characterization and neuropharmacological assessments. Drug Development and Industrial Pharmacy. 2021; 47: 12–21.
[31] Devangan P, Saini A, Patel D, Kolhe U. Solubility Enhancement of Aripiprazole via Mesoporous Silica: Preparation, Characterization, *In vitro* Drug Release, and Solubility Determination. Journal of Pharmaceutical Innovation. 2023; 18: 1316–1327.
[32] Thakral NK, Zanon RL, Kelly RC, Thakral S. Applications of Powder X-Ray Diffraction in Small Molecule Pharmaceuticals: Achievements and Aspirations. Journal of Pharmaceutical Sciences. 2018; 107: 2969–2982.
[33] Zappi A, Maini L, Galimberti G, Caliandro R, Melucci D. Quantifying API polymorphs in formulations using X-ray powder diffraction and multivariate standard addition method combined with net analyte signal analysis. European Journal of Pharmaceutical Sciences. 2019; 130: 36–43.
[34] Hoyos-Montilla AA, Puertas F, Molina Mosquera J, Tobón JI. Infrared spectra experimental analyses on alkali-activated fly ash-based binders. Spectrochimica Acta. Part A, Molecular and Biomolecular Spectroscopy. 2022; 269: 120698.
[35] An JH, Kiyonga AN, Yoon W, Ryu HC, Kim JS, Kang C, *et al*. Crystal Structure Analysis of the First Discovered Stability-Enhanced Solid State of Tenofovir Disoproxil Free Base Using Single Crystal X-ray Diffraction. Molecules. 2017; 22: 1182.
[36] Uri A, Bezaatpour A, Amiri M, Vucetic N, Mikkola JP, Murzin DY. Pd Nanoparticles Stabilized on the Cross-Linked Melamine-Based SBA-15 as a Catalyst for the Mizoroki–Heck Reaction. Catalyst Letters. 2022; 152: 991–1002.
[37] Zauška Ľ, Beňová E, Urbanová M, Brus J, Zeleňák V, Hornebecq V, *et al*. Adsorption and Release Properties of Drug Delivery System Naproxen-SBA-15: Effect of Surface Polarity, Sodium/Acid Drug Form and *pH*. Journal of Functional Biomaterials. 2022; 13: 275.
[38] Gkiliopoulos D, Tsamesidis I, Theocharidou A, Pouroutzidou GK, Christodoulou E, Stalika E, *et al*. SBA-15 Mesoporous Silica as Delivery Vehicle for rhBMP-2 Bone Morphogenic Protein for Dental Applications. Nanomaterials. 2022; 12: 822.
[39] Nainwal N, Singh R, Jawla S, Saharan VA. The Solubility-Permeability Interplay for Solubility-Enabling Oral Formulations. Current Drug Targets. 2019; 20: 1434–1446.
[40] Kaur N, Suryanarayanan R. Levothyroxine Sodium Pentahydrate Tablets - Formulation Considerations. Journal of Pharmaceutical Sciences. 2021; 110: 3743–3756.
[41] Liu X, Zhao L, Wu B, Chen F. Improving solubility of poorly water-soluble drugs by protein-based strategy: A review. International Journal of Pharmaceutics. 2023; 634: 122704.
[42] Tiwari R, Siddiqui MH, Mahmood T, Farooqui A, Tiwari M, Shariq M, *et al*. Solubility enhancement of curcumin, quercetin and rutin by solid dispersion method. Annals of Phytomedicines. 2021; 10: 462–471.
[43] Chaudhary N, Tripathi D, Rai AK. A Technical Approach of Solubility Enhancement of Poorly Soluble Drugs: Liquisolid Technique. Current Drug Delivery. 2020; 17: 638–650.
[44] Vallet-Regí M, Schüth F, Lozano D, Colilla M, Manzano M. Engineering mesoporous silica nanoparticles for drug delivery: where are we after two decades? Chemical Society Reviews. 2022; 51: 5365–5451.
[45] Zhao Z, Ukidve A, Kim J, Mitragotri S. Targeting Strategies for Tissue-Specific Drug Delivery. Cell. 2020; 181: 151–167.
[46] Esperanza Adrover M, Pedernera M, Bonne M, Lebeau B, Bucalá V, Gallo L. Synthesis and characterization of mesoporous SBA-15 and SBA-16 as carriers to improve albendazole dissolution rate. Saudi Pharmaceutical Journal. 2020; 28: 15–24.
[47] Ulfa M, Prasetyoko D. Drug loading-release behaviour of mesoporous materials SBA-15 and CMK-3 using ibuprofen molecule as drug model. Journal of Physiologist Conference Services. 2019; 1153: 012065.
[48] Ekenna IC, Abali SO. Comparison of the Use of Kinetic Model Plots and DD Solver Software to Evaluate the Drug Release from Griseofulvin Tablets. Pharmaceutical Sciences and Inventions. 2022; 12: 3–5.
[49] Abdul Rasool BK, Sammour R. DDSolver Software Application for Quantitative Analysis of In vitro Drug Release Behavior of the Gastroretentive Floating Tablets Combined with Radiological Study in Rabbits. Current Drug Delivery. 2022; 19: 949–965.
[50] Thanawuth K, Limmatvapirat S, Rojviriya C, Sriamornsak P. Controlled Release of Felodipine from 3D-Printed Tablets with Constant Surface Area: Influence of Surface Geometry. Pharmaceutics. 2023; 15: 467.
[51] Khalid R, Nasiri MI, Sarwar H, Yasmin R, Zaheer K, Anwer S, *et al*. Influence of cellulose and acetate-based polymers on the release of ciprofloxacin HCl from extended release matrix tablets prepared by direct compression technique. Bulletin of Pharmaceutical Sciences. 2020; 43: 11–25.
[52] Dadej A, Woźniak-Braszak A, Bilski P, Piotrowska-Kempisty H, Józkowiak M, Pawełczyk A, *et al*. Improved solubility of lornoxicam by inclusion into SBA-15: Comparison of loading methods. European Journal of Pharmaceutical Sciences. 2022; 171: 106133.
[53] Trzeciak K, Chotera-Ouda A, Bak-Sypien II, Potrzebowski MJ. Mesoporous Silica Particles as Drug Delivery Systems-The State of the Art in Loading Methods and the Recent Progress in Analytical Techniques for Monitoring These Processes. Pharmaceutics. 2021; 13: 950.

[54] Tian Y, Wang S, Yu Y, Sun W, Fan R, Shi J, *et al*. Review of nanosuspension formulation and process analysis in wet media milling using microhydrodynamic model and emerging characterization methods. International Journal of Pharmaceutics. 2022; 623: 121862.

[55] Ling JKU, Chan YS, Nandong J. Insights into the release mechanisms of antioxidants from nanoemulsion droplets. Journal of Food Science and Technology. 2022; 59: 1677–1691.

[56] Liu M, Svirskis D, Proft T, Loh JMS, Wen J. Preformulation studies of thymopentin: analytical method development, physicochemical properties, kinetic degradation investigations and formulation perspective. Drug Development and Industrial Pharmacy. 2021; 47: 1680–1692.

[57] Dadej A, Woźniak-Braszak A, Bilski P, Piotrowska-Kempisty H, Józkowiak M, Stawny M, *et al*. APTES-Modified SBA-15 as a Non-Toxic Carrier for Phenylbutazone. Materials. 2022; 15: 946.

[58] Paarakh MP, Jose PA, Setty CM, Christoper GVP. Release kinetics - concept and applications. International Journal of Pharmaceutical Research and Technology. 2019; 8: 12–20.

[59] Mitchell MJ, Billingsley MM, Haley RM, Wechsler ME, Peppas NA, Langer R. Engineering precision nanoparticles for drug delivery. Nature Reviews. Drug Discovery. 2021; 20: 101–124.

[60] Jung YH, Heo DG, Lee DC, Kwon YM, Seol MJ, Zhang D, *et al*. Effect of concomitant oral administration of ethanol on the pharmacokinetics of nicardipine in rats. Biomedical Chromatography. 2022; 36: e5425.